AIMS Biophysics

AIMS Biophysics, 12(1): 54−68.
DOI: 10.3934/biophy.2025005
Received: 22 January 2025
Revised: 25 February 2025
Accepted: 05 March 2025
Published: 11 March 2025

http://www.aimspress.com/journal/biophysics

Research article

Tissue-specific bioimpedance changes induced by graphene oxide *ex vivo*: a step toward contrast media development

Svetlana Kashina[1,*], Andrea Monserrat del Rayo Cervantes-Guerrero[1], Francisco Miguel Vargas-Luna[1], Gonzalo Paez[2] and Jose Marco Balleza-Ordaz[1,*]

[1] Division of Sciences and Engineering, University of Guanajuato. Loma del Bosque 103, Lomas del Campestre CP 37150. Leon, Guanajuato, México
[2] Center for Optics Research, Loma del Bosque 115, Colonia Lomas del Campestre León, Guanajuato, México. Código Postal 37150

* **Correspondence:** Email: jm.balleza@ugto.mx; Tel: +524777885100.

Abstract: Electrical bioimpedance (BI) was proposed as an easy and cheap technique to monitor different physiological parameters. However, its clinical applications are minimal due to the low resolution and difficulties in discriminating between different tissue types. Nanoparticles have also been extensively investigated for their practical use. Graphene oxide (GO) has shown acceptable biocompatibility. The objective of this work was to assess the possibility of using GO to enhance bioimpedance measures in ex vivo models. GO was suspended in medical-grade solutions and injected into the tissues. BI was recorded at 12.5, 25, 50, and 100 kHz. Bode impedance plots evidenced statistically significant differences in tissue impedance before and after injections. Likewise, data adjustment to an equivalent electrical circuit showed that GO accumulates mainly in the extracellular space and, to some extent, at the cytoplasmatic membrane, and the accumulation is tissue specific. The latter suggests the possibility of using GO as a contrast agent to discriminate between different tissue types using BI.

Keywords: graphene oxide; bioimpedance; porcine organs; tissue electrical properties; contrast media

1. Introduction

Bioimpedance (BI) is a noninvasive technique that is used to determine body composition.

Different research groups have also proposed BI to monitor and quantify other physiological functions, such as pulmonary, cardiac, or gastric [1]. Briefly, the technique consists of injecting a small-amplitude alternative current (AC) and detecting the electric potential.

Bioimpedance spectroscopy has become an important tool in body composition analysis, widely used in wearable devices to monitor fat mass, lean mass, and hydration levels with high accuracy [2]. Integrating BI into tissue engineering enables non-invasive real-time monitoring of cell viability and differentiation in engineered constructs without the need for disruptive testing [3]. Portable bioimpedance systems, enhanced by machine learning, are emerging as point-of-care tools for fluid status monitoring in dialysis patients and early detection of conditions like lymphedema [4].

BI measurements can be obtained using different frequencies, performing electrical impedance spectroscopy (EIS). EIS increases resolution and provides more information about the properties of biological materials and pathophysiological processes than single-frequency BI [5,6]. However, due to the internal characteristics of EIS and the basic use of circuit-based mathematical model, there are errors in measurement, which limit the practical use of this technology. For this reason, many research groups are working on different methodologies to correct errors based on equipment design and signal processing [7].

Our research group proposes a new approach to enhance BI and EIS through the previous application of a contrast media to the studied tissue or organism. It is known that many clinical diagnostic methods such as MRI and radiology benefit from contrast media [8]. Nevertheless, the possibility of contrast media use for BI studies has not been investigated. Nevertheless, the possibility of contrast media use for BI studies has not been investigated. The investigation supports the growing need to improve BI's sensitivity, making it a more competitive alternative to traditional imaging modalities like MRI or CT which rely on established contrast agents [9].

There are some reports regarding the use of the saline solution in lung electrical impedance tomography (EIT) [10,11], however, the saline solution is not specific and does not allow discrimination between different tissue types. In our previous work, it has been shown that the injection of crystal solutions can improve the differentiation between tissue types [12], however, possibly adding some semiconductor materials may lead to better results.

On the other hand, different nanoparticles (NPs) have been proposed as contrast agents for different imaging techniques [13]. NPs can be manufactured from different materials, including conductive and semiconductive materials, and modified to target specific tissues and cell types (for example, by adding specific antibodies) [14]. Despite the advances in their use as contrast agents, NPs' potential to be used in BI studies has not been explored. Additionally, the obtained parameters can be used to sense the accumulation of nanoparticles in concentrations potentially harmful to the organism.

Graphene oxide (GO) is a 2D nanostructured semiconductive material with acceptable biocompatibility [15]. Due to the presence of functional groups, GO can be modified with aptamers and other molecules to increase its specificity [16,17]. Additionally, GO has been proposed as a multifunctional platform for imaging and other purposes [18]. Unlike graphene, GO presents different hydrophilic functional groups that augment its solubility and biocompatibility and may serve as linking agents for other functional molecules. Nevertheless, these functional groups disturb perfect sp^2 configuration by introducing gaps, thus disrupting π-π interactions and influencing the electrical properties of GO. Casero et al. (2012) determined electrochemically that the charge transfer resistance of GO is four times greater than that for electrochemically reduced graphene (95.45 and 21.07 Ohm/cm^2, respectively) [19]. The resistance of the GO solution is inversely proportional to its

concentration, but the capacitance seems to be independent of the GO concentration [20].

EIS serves as a valuable tool in elucidating the properties of GO-modified electrodes. Through EIS, several key properties of GO can be determined. First, EIS provides insights into the electrical conductivity of GO films or composites by analyzing their impedance spectra. Changes in conductivity due to factors such as oxygen functional groups, defects, or doping can be discerned, influencing charge transfer processes at the electrode–electrolyte interface [21]. Second, EIS allows for the investigation of ion diffusion kinetics within GO-based materials, providing information on their porosity, surface area, and ion transport pathways. Moreover, EIS can reveal interfacial phenomena, such as adsorption/desorption processes and double-layer capacitance, shedding light on the interactions between GO and electrolytes [22]. Overall, by employing EIS, it is possible to characterize the electrochemical properties of GO and tailor its structure and composition for a wide range of applications, from energy storage to sensing.

For all the properties mentioned above, we hypothesize that GO may be used as a contrast agent in bioimpedance studies, potentializing the effect of crystalloid solutions. In this work, we assess the capability of GO to modify the electrical properties of ex vivo biological tissues to provide the proof of concept.

2. Materials and methods

2.1. Graphene oxide synthesis and solutions

GO was synthesized from pure graphite rod using the conventional Hummers method [23]. NaCl (0.9%) and Hartmann medical-grade solutions (both PiSA Pharmaceutica, Mexico) were used to dissolve GO. Hartmann solution contained the following ions: sodium, 131 mmol/L, chloride, 111 mmol/L, lactate, 29 mmol/L, potassium, 5 mmol/L, and calcium, 4 mmol/L.

2.2. GO characterization

TEM was performed using a JEM-1010 electron microscope (GATAN, CA, USA). DXR™ Raman microscope (Thermo Fisher Scientific, USA) was used to obtain Raman spectra.

2.3. Ex vivo tissue samples

The porcine model was chosen for the study due to its resemblance to the human tissues and organs, so, the obtained data would be more significant to the field [24]. Porcine liver, brain, and kidney were freshly purchased at the local market on the same day the study was performed. Careful visual inspection was conducted for each organ to ensure the absence of damaged tissue, then, each organ was washed and cut into 8 g pieces.

2.4. Bioimpedance data acquisition

BI studies were performed using a BIOPAC system coupled with The EBI100C electrobioimpedance amplifier (BIOPAC Systems Inc., CA, USA). BIOPAC injects an electrical current of 400 μA at preset 12.5, 25, 50, and 100 kHz frequencies using the tetrapolar electrode method.

These frequencies were chosen because they are within the beta dispersion region and are commonly used for human-based applications [25]. In the study, a sampling rate of 1000 samples/second was used. A linear arrangement of 4 stainless steel medical needles with 1 cm of distance between them was used as electrodes. 0.5 mg/mL GO solutions in Hartmann and Saline solutions were prepared. Tissue samples were injected with 1 mL of each solution separately, including Hartmann and Saline solution as controls. Immediately after, BI measurements were acquired for 1 min. The procedure was performed three times in triplicate for each study condition. The data was recorded for 1 min for each frequency to allow the system to be settled and the data from the last second was recorded. Additionally, BI was assessed for pristine solutions. The data obtained was recorded in the database and stored for analysis.

2.5. Data analysis and statistics

All data vectors were assessed using Kolmogorov-Smirnov statistical test. Since all data evidenced normal distribution, it was presented as mean ± SD. Data for the BI module and phase were treated separately. Students' t-test for independent data was used. Unless the contrary is stated, all differences were statistically significant ($p < 0.05$). The significant level was set at $p < 0.05$.

The standard Debye model was used to fit the bioimpedance data [26]. The bioimpedance data was adjusted to the function represented with a real and an imaginary part, as follows:

$$Z = \frac{R_I R_E (R_I + R_E) + (X)^2 R_E}{(R_I + R_E)^2 + (X)^2} - j \frac{X(R_E (R_I + R_E) - R_I R_E)}{(R_I + R_E)^2 + (X)^2} \quad (1)$$

Where Ri stands for extracellular resistance, Re for extracellular resistance, and X for the capacitance factor that is calculated as in (2).

$$X = \frac{1}{2 * \pi * C} \quad (2)$$

Where C is the capacitance of the membrane.

3. Results and discussion

The BI data followed a normal distribution, it was treated as mean ± SD, however, SD in all cases was significantly smaller than mean values (magnitudes of 10^{-2}–10^{-1}). For that reason, SD cannot be appreciated on the graphics.

First, the characterization of the obtained GO was performed. Figure 1 presents a TEM image of the obtained GO. A mixture of different-shaped thin particles can be observed, indicating that the obtained GO is a 2D material, as expected as a result of the synthesis. Additionally, the particle's size was relatively small, which may present an advantage.

In Raman spectra (Figure 2), two peaks can be observed: at 1320 and 1590 cm^{-1}, corresponding to D and G bands, respectively. The G band in carbon materials is linked to sp^2 vibrations, while the D band is linked to defections. The G/D ratio corresponds to the crystallinity rate [27]. For GO obtained in this study, the ratio was 27%, indicating that the sp^2 was indeed distorted by functional group formation.

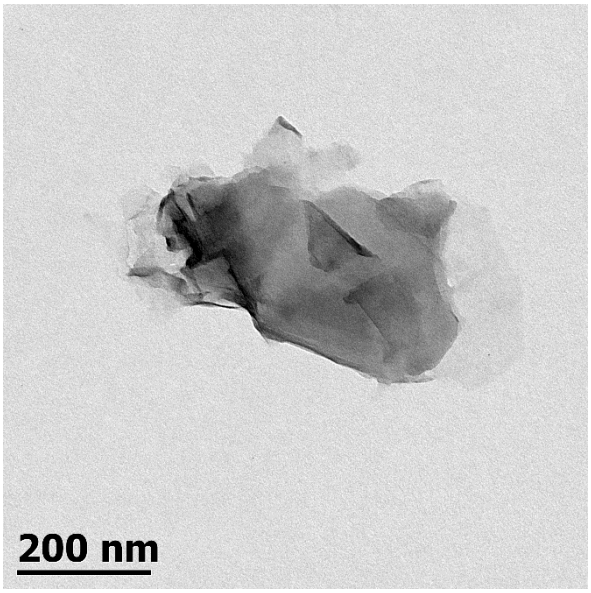

Figure 1. TEM image of obtained graphene oxide.

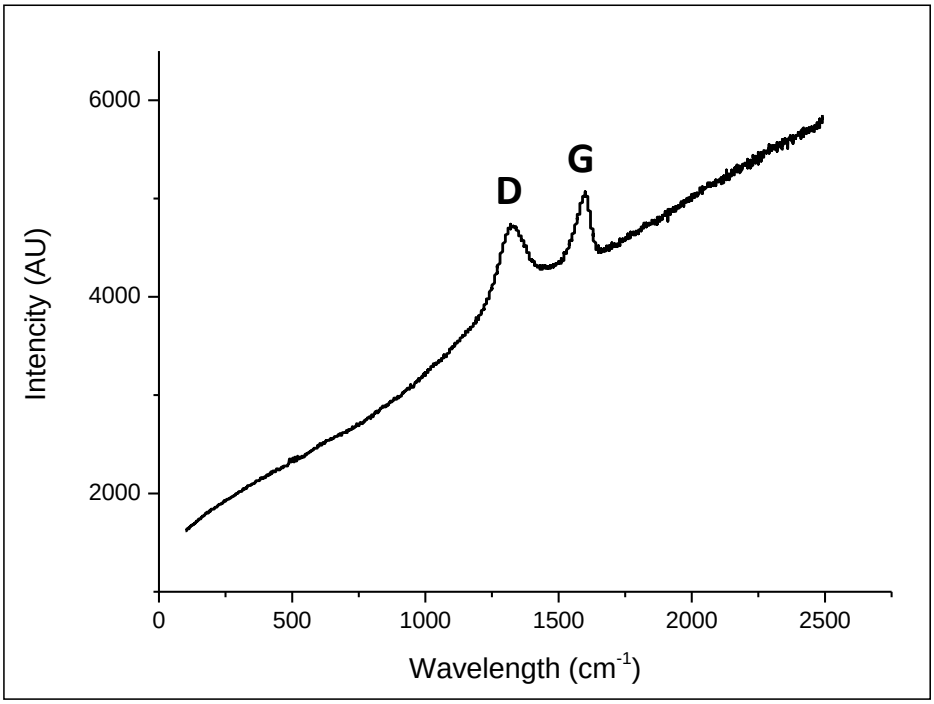

Figure 2. Raman spectra obtained for GO.

Figure 3 represents FTIR spectra obtained for GO. The presence of several functional groups can be seen. The strong broad peak at approximately 3430 cm^{-1} corresponds to alcohol group –O–H stretching, which is typical for GO. Two small peaks at 3000–2840 cm^{-1} and a medium peak at 1372 cm^{-1} can be attributed to –C–H stretching of alkane, which means that some parts of the GO have lost aromaticity. This finding is consistent with Raman spectra analysis of the GO crystallinity. The weak

peak at 1917 cm^{-1} is assigned to –C–H bending in aromatic compounds, thus confirming that some sp^2 structures of graphite were conserved after GO synthesis. The ketone and/or carboxylic acid group –C=O stretching peak is observed at 1711 cm^{-1}, indicating the presence of oxidated groups. The medium peak at 1573 cm^{-1} is typical of cyclic alkene C=C stretching. Also, FTIR spectra show that an oxidation process of graphite occurred, and the results are consistent with the low crystallinity obtained by Raman.

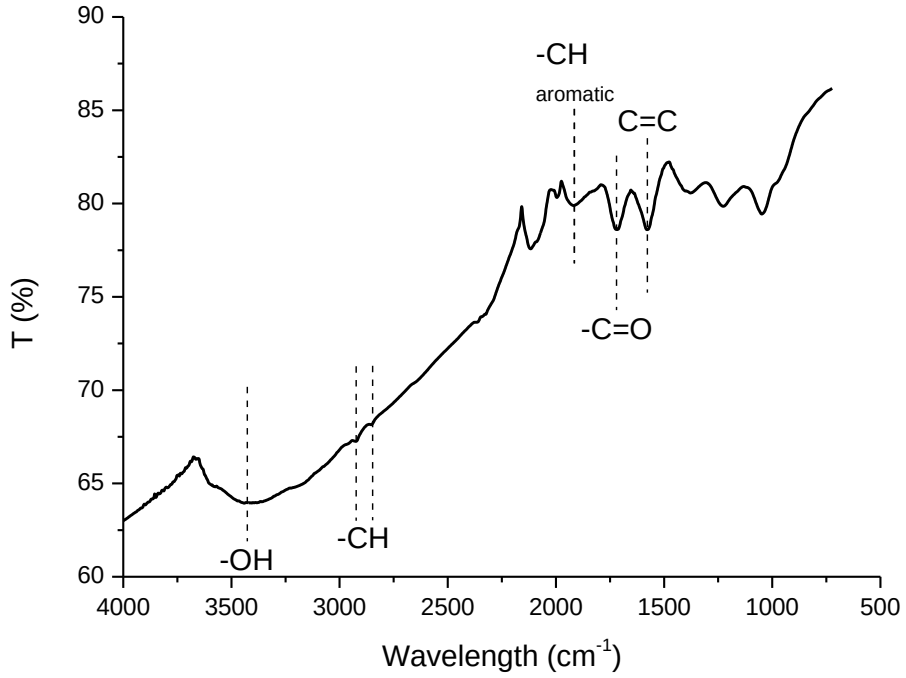

Figure 3. FTIR spectra obtained for GO.

As mentioned in the introduction, BI studies are noninvasive, cheap, and radiation-free. However, their applications are limited due to difficulties in discriminating between tissue types. In 2002 Frerichs et al [28] applied a hypertonic saline solution to improve EIT imaging. The results were positive but the technique was not adopted by clinicians due to possible complications of hypertonic saline solution on patients. Hellige et al. (2012) [29] investigated the effect of radiographic contrast media in EIT in vitro. The results were also encouraging, but as in the case of hypertonic saline solution, the work was not followed up in models or patients. For BI, no such studies were conducted, so, to the authors' knowledge, this is the first attempt to apply nanomaterials as possible contrast media for BI studies.

Taking that into account, the study was conducted with carefully chosen controls. Figure 4 shows BI data obtained for Hartmann, saline, and GO solutions. It can be observed that the saline solution presented a lower resistance to charge transfer than the Hartmann solution at all studied frequencies. GO addition augmented the impedance module, which is logical since GO is a semiconductor. On the other hand, the impedance phase for the Hartmann solution was almost zero at the studied frequencies, and GO addition did not change this significantly. For NaCl, the observed phase was slightly negative, probably due to the double-layer capacitance formed on the interface between the solution and the electrodes. GO addition in both solutions set the phase roughly to zero, indicating that there was an interaction between the material and the ions, making them less available for double-layer formation.

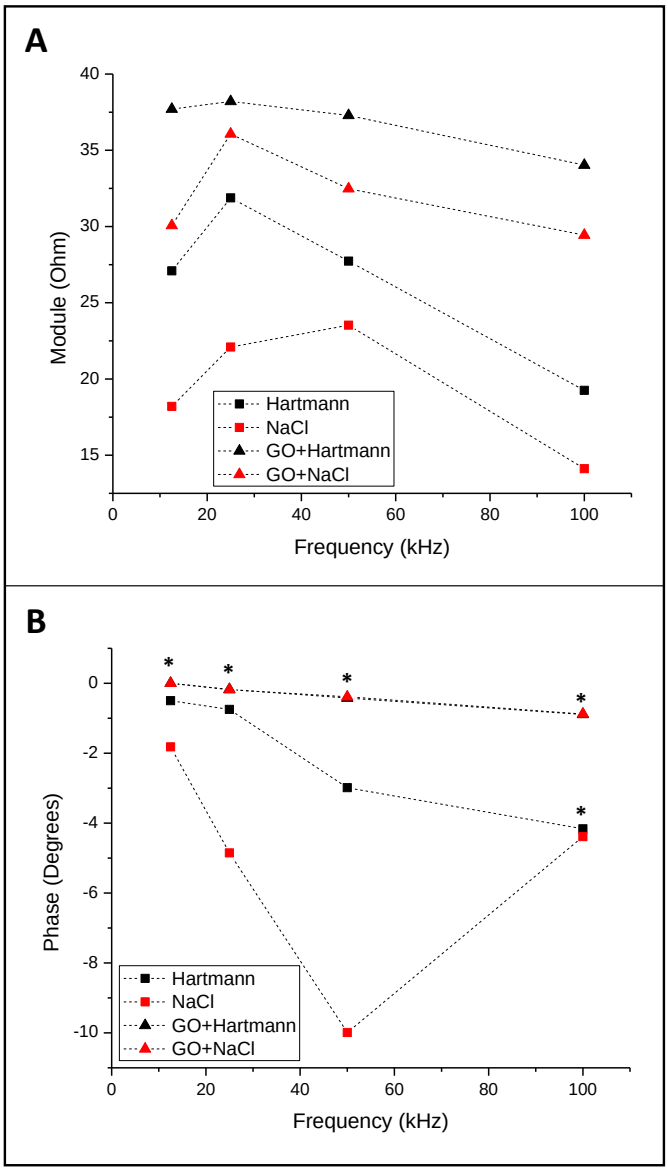

Figure 4. Bode graphs obtained for the crystalloid solutions and GO. A) Impedance module and B) Impedance phase (* indicates that there were no statistically significant differences between conditions).

Three types of tissue were included in the study: liver, kidney, and brain. The first two were chosen because all exogenous substances eventually will be excreted from an organism via one or both organs, so the probability of their accumulation in the organs is high. Additionally, the brain was chosen to evaluate possible GO accumulation.

In previous studies, it was shown that pristine GO can be accumulated in the liver [30]; hence, it can be detected and can highlight BI information from the organ. Figure 5 presents the results obtained for GO and crystalloid solutions as controls. The resistance value of the human liver was estimated as 342 Ohm (296–396 Ohm, 95% confidence interval) [31]. The highest value obtained for porcine organs was 220 Ohm at 12.5 kHz, which is relatively close to the human value. Phase analysis (Figure 5B) indicates that at the studied frequencies, the liver presented a slightly capacitive behavior and did not vary greatly in the presence of solutions or GO. On the other hand, the impedance module presented

significant changes, especially at 12.5 kHz. The differences cannot be attributed only to the solutions but to GO addition as well. This finding is interesting because it can be used to increase the resolution of EIT-based techniques, as in the case of liver fat content determination [32].

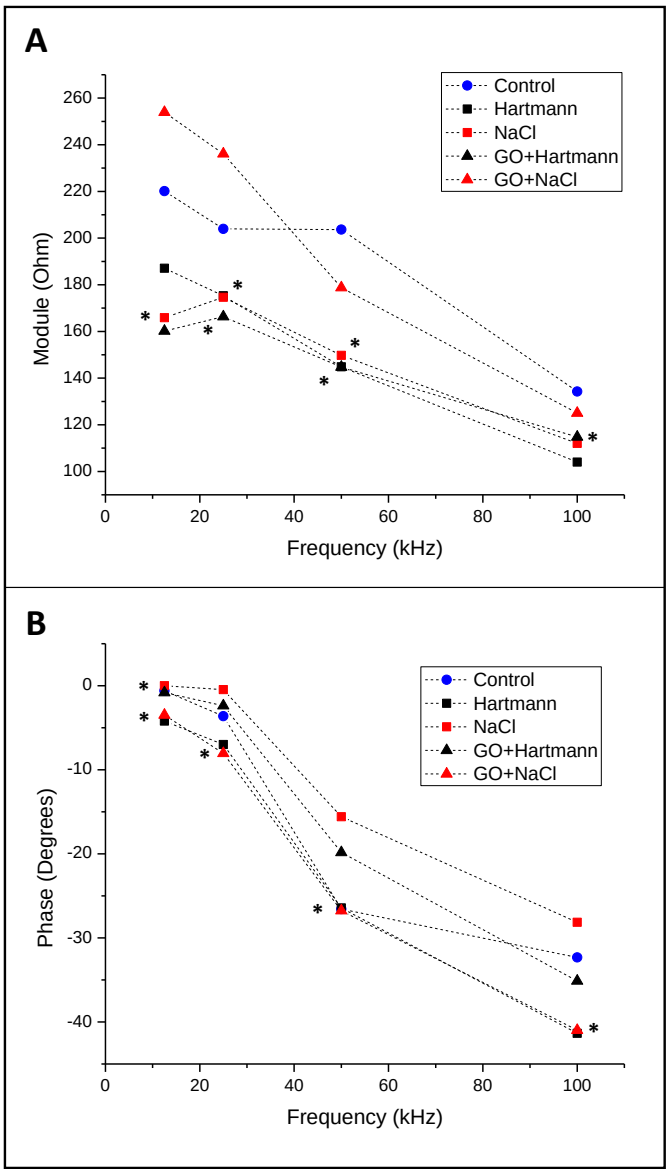

Figure 5. Bode graphs for porcine liver. A) Impedance module; B) Impedance phase (* indicates that there were no statistically significant differences between conditions).

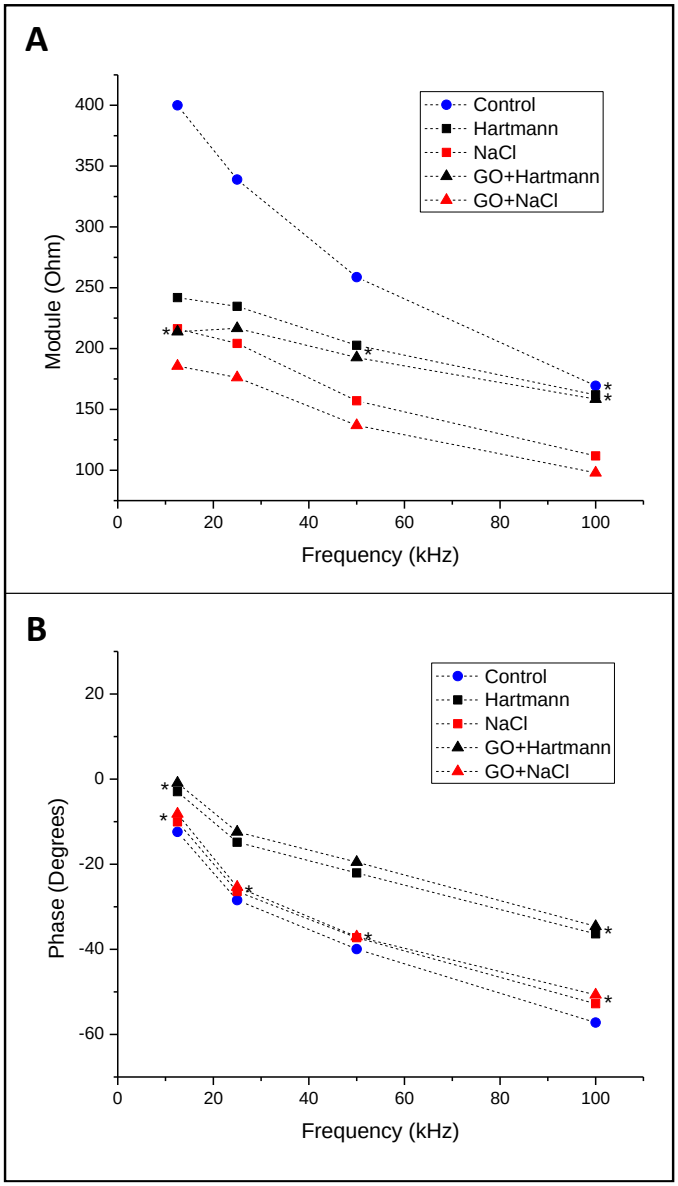

Figure 6. Bode plot for data obtained for porcine kidney. A) Impedance module; B) Impedance phase (* indicates that there were no statistically significant differences between conditions).

Another possible route to eliminate nanoparticles from the organism is through the urinary tract. Since GO is hydrophilic, its elimination may be carried out through glomerular filtration. It has been shown that GO does not affect kidney function, and full barrier function is restored after 48 h of exposure [33]. Figure 6 shows the Bode plots obtained for kidney tissue. The resistance of human kidneys is estimated to be 211 Ohm [31]. A 180–390 Ohm range was obtained for the porcine organ, which is comparable to the previously reported value. As for the liver, the module at 12.5 kHz presented better resolution between before and after GO injection. GO increases the tissue conductivity, thus making it more distinguishable from adjacent tissue. The impedance phase presented more significant changes at 100 kHz. However, differences may not be attributed to GO since the results are not statistically different from those obtained for solutions alone.

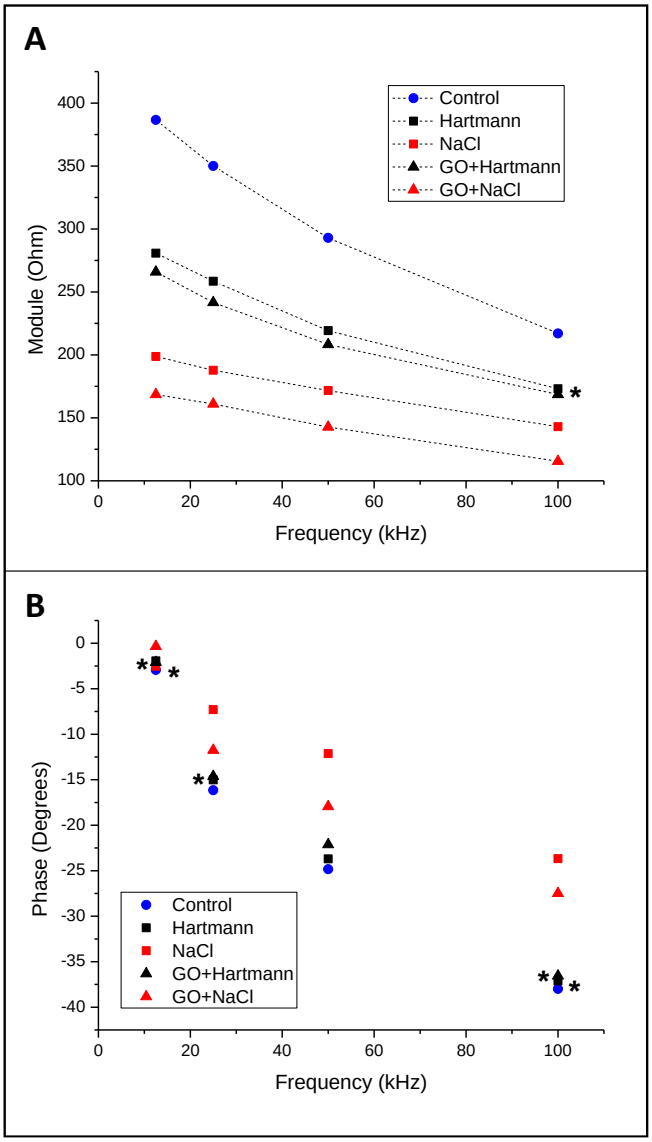

Figure 7. Bode plots obtained for the porcine brain: A) Impedance module; B) Impedance phase (* indicates that there were no statistically significant differences between conditions).

In addition to organs dedicated to excretion, a nervous tissue (brain) was analyzed. The electrical resistance of the brain tissue varies greatly in the literature: from 50 Ohms [34] to 2976 Ohms [35], depending on the studied species, frequency range, and other experimental conditions. In this work, 217−387 Ohm resistance was obtained (Figure 7), which is lower than some previous results. We offer two possible explanations for this fact. First, the majority of studies report DC and AC at low frequencies; in this work, AC was used, and the frequencies used were significantly higher, so it is possible that at the studied conditions, the brain tissue was more conductive. Secondly, studies where the highest resistance was obtained were conducted in living organisms. Likely, ex vivo tissues do not retain strong endothelium junctions, thus allowing more easy charge flow and lowering tissue resistance.

Like the other studied organs, a tissue resistance decrease induced by GO may be observed at 12.5 kHz,

being highest in NaCl solution. On the other hand, in this case, the phase presented significant differences at 100 kHz when GO was added, which indicates that capacitive behavior is diminished, probably due to an interaction between the cell membrane and GO. These two parameters—module change at 12.5 kHz and phase change at 100 kHz—may be potentially beneficial for electrochemical studies of the blood–brain barrier, since its resistance may reach 1500 Ohm [36].

We obtained differences in impedance modules are generally lower for all tissues studied. This fact is consistent with the previous findings [10], in which the relative impedance of lung tissue was lower after injection of the saline solution.

The obtained data were adjusted to the equivalent electrical circuit shown in Figure 8 to perform a more in-depth analysis. This is a minimum model that considers both intracellular and extracellular resistance and membrane capacitance; thus, GO effects on these parameters may be estimated.

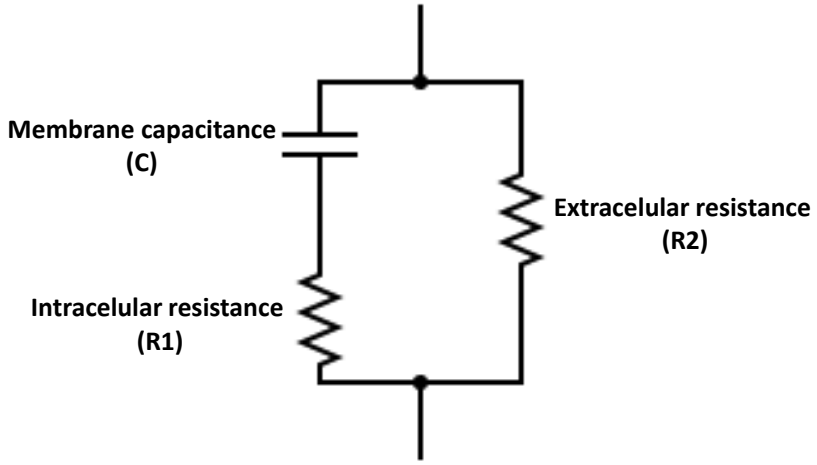

Figure 8. Equivalent electrical circuit.

Table 1 presents parameters obtained by nonlinear regression. It can be seen that the R^2 for all adjustments was higher than 0.95, which indicates that the obtained coefficients represent the data correctly. For the liver, a very small capacitance change was obtained, indicating no effect on the cellular membrane. On the contrary, the resistance values changed, indicating that GO accumulated in both compartments. It is unclear why GO in the Hartmann solution reduces R1 and R2. Probably, this behavior is due to an interaction between the liver cell's components, ions of the crystalloid solution, and GO. The kidney showed a clearer pattern of GO accumulation in the extracellular space, and, in NaCl, accumulated at the membrane, as the change in capacitance indicates. It is likely that brain cell membranes also accumulate GO, increasing their capacitance, and in the extracellular space, as R2 changes suggest. However, it is clear that the obtained difference was, in general, better for NaCl. It is probable that ions from the Hartmann solution interact with GO, thus canceling its superficial charges and lowering its ability to interact with the cells. Nevertheless, in vivo studies should be conducted to confirm the in-cell distribution.

While encouraging results have been achieved, some limitations are worth mentioning. It is possible that GO could lead to inconsistent results in certain organs, potentially complicating bioimpedance (BI) interpretations. Also, the alteration of electrical properties by GO in tissues might introduce unintended side effects, such as interference with normal physiological functions,

particularly in unstudied biological contexts. It is necessary to perform *in vivo* validation to assess GO toxicity or adverse reactions when applied to living organisms.

Table 1. Estimated parameters of the equivalent circuit.

	R1 (Ohm)	R2 (Ohm)	C (nF)	R^2
		Liver		
Control	32	219	7	0.95
GO in Hartmann	14	167	8	0.97
GO in NaCl	52	268	9	0.996
		Kidney		
Control	53	420	9	0.993
GO in Hartmann	60	219	6	0.996
GO in NaCl	38	194	14	0.999
		Brain		
Control	152	397	5.5	0.996
GO in Hartmann	157	272	7	0.994
GO in NaCl	128	171	8	0.999

4. Conclusions

In this study, we evaluated the potential of using graphene oxide (GO) to enhance the differentiation of tissue types, as a preliminary step toward developing contrast media for bioimpedance (BI) studies. Our findings demonstrated that, in ex vivo models, GO alters the electrical properties of tissues, enabling the use of single-frequency BI or BI spectroscopy to detect GO accumulation. The observed changes in BI were specific to the tissue type, a key factor for its potential application as a contrast medium. However, while our hypothesis posited that GO could improve tissue discrimination, the results confirmed this effect only within the specific organs examined, highlighting a tissue-dependent response. This suggests that the efficacy of GO as a contrast agent may vary across different biological contexts. The current findings are thus limited to the studied organs, and further, in vivo studies are necessary to validate these outcomes and assess the broader applicability of GO in BI-based contrast media development.

Use of generative-AI tools declaration

The authors declare they have not used Artificial Intelligence (AI) tools in the creation of this article.

Acknowledgments

Svetlana Kashina thanks SECIHTI Mexico for postdoctoral fellowship.

Conflict of interest

The authors declare no conflict of interest. The study was approved by the institutional ethics

committee (approval number: CEPIUG-A01-2022).

Author contributions

Svetlana Kashina: Conceptualization, Formal analysis, Funding acquisition, Methodology, Project administration, Supervision, Investigation, Writing–original draft; Andrea Monserrat del Rayo Cervantes-Guerrero: Data acquisition and curation, Formal analysis, Writing–review & editing; Francisco Miguel Vargas-Luna: Formal analysis, Investigation, Resources, Validation, Writing–review; Gonzalo Paez: Conceptualization, Formal analysis, Funding acquisition, Methodology, Project administration, Supervision, Writing–review & editing; Jose Marco Balleza-Ordaz: Formal analysis, Investigation, Resources, Validation, Writing–review & editing.

Data access statement

The data associated with this work will be made available upon reasonable request.

References

1. Simini F, Bertemes-Filho P (2018) *Bioimpedance in Biomedical Applications and Research*, New York: Springer. https://doi.org/10.1007/978-3-319-74388-2
2. Aldobali M, Pal K (2021) Bioelectrical impedance analysis for evaluation of body composition: a review. *2021 International Congress of Advanced Technology and Engineering (ICOTEN)*, 1−10. https://doi.org/10.1109/ICOTEN52080.2021.9493494
3. Amini M, Hisdal J, Kalvøy H (2018) Applications of bioimpedance measurement techniques in tissue engineering. *Electr Bioimpedance* 9: 142−158. https://doi.org/10.2478/joeb-2018-0019
4. Lukaski HC, Vega Diaz N, Talluri A, et al. (2019) Classification of hydration in clinical conditions: indirect and direct approaches using bioimpedance. *Nutrients* 11: 809. https://doi.org/10.3390/nu11040809
5. Sanchez B, Vandersteen G, Martin I, et al. (2013) In vivo electrical bioimpedance characterization of human lung tissue during the bronchoscopy procedure. A feasibility study. *Med Eng Phys* 35: 949–957. https://doi.org/10.1016/j.medengphy.2012.09.004
6. Sanchez B, Louarroudi E, Jorge E, et al. (2013) A new measuring and identification approach for time-varying bioimpedance using multisine electrical impedance spectroscopy. *Physiol Meas* 34: 339. https://doi.org/10.1088/0967-3334/34/3/339
7. Subhan S, Ha S (2019) A harmonic error cancellation method for accurate clock-based electrochemical impedance spectroscopy. *IEEE T Biomed Circ S* 13: 710–724. https://doi.org/10.1109/TBCAS.2019.2923719
8. Schöckel L, Jost G, Seidensticker P, et al. (2020) Developments in X-ray contrast media and the potential impact on computed tomography. *Invest Radiol* 55: 592–597. https://doi.org/10.1097/RLI.0000000000000696
9 Naranjo-Hernández D, Reina-Tosina J, Min M (2019) Fundamentals, recent advances, and future challenges in bioimpedance devices for healthcare applications. *J Sensors* 201: 9210258. https://doi.org/10.1155/2019/9210258

10. Sobota V, Müller M, Roubík K (2019) Intravenous administration of normal saline may be misinterpreted as a change of end-expiratory lung volume when using electrical impedance tomography. *Sci Rep* 9: 5775. https://doi.org/10.1038/s41598-019-42241-7
11. Putensen C, Hentze B, Muenster S, et al. (2019) Electrical impedance tomography for cardio-pulmonary monitoring. *J Clin Med* 8: 1176. https://doi.org/10.3390/jcm8081176
12. Cervantes A, Paez G, Balleza-Ordaz JM, et al. (2024) Electrical bioimpedance analysis and comparison in biological tissues through crystalloid solutions implementation. *Biosens Bioelectron* 246: 115874. https://doi.org/10.1016/j.bios.2023.115874
13. Avasthi A, Caro C, Pozo-Torres E, et al. (2020) Magnetic nanoparticles as MRI contrast agents, *Surface-modified Nanobiomaterials for Electrochemical and Biomedicine Applications*, Springer, Cham, 49–91. https://doi.org/10.1007/978-3-030-55502-3_3
14. Thakur A, Thakur P, Khurana SP (2022) *Synthesis and Applications of Nanoparticles*, Singapore: Springer. https://doi.org/10.1007/978-981-16-6819-7
15. Liao C, Li Y, Tjong SC (2018) Graphene nanomaterials: synthesis, biocompatibility, and cytotoxicity. *Int J Mol Sci* 19: 3564. https://doi.org/10.3390/ijms19113564
16. Sekhon SS, Kaur P, Kim YH, et al. (2021) 2D graphene oxide–aptamer conjugate materials for cancer diagnosis. *Npj 2D Mater Appl* 5: 21. https://doi.org/10.1038/s41699-021-00202-7
17. Huang A, Zhang L, Li W, et al. (2018) Controlled fluorescence quenching by antibody-conjugated graphene oxide to measure tau protein. *Roy Soc Open Sci* 5: 171808. https://doi.org/10.1098/rsos.171808
18. Campbell E, Hasan M, Pho C, et al. (2019) Graphene oxide as a multifunctional platform for intracellular delivery, imaging, and cancer sensing. *Sci Rep* 9: 416. https://doi.org/10.1038/s41598-018-36617-4
19. Casero E, Parra-Alfambra A, Petit-Domínguez M, et al. (2012) Differentiation between graphene oxide and reduced graphene by electrochemical impedance spectroscopy (EIS). *Electrochem Commun* 20: 63–66. https://doi.org/10.1016/j.elecom.2012.04.002
20. Yoon Y, Jo J, Kim S, et al. (2017) Impedance spectroscopy analysis and equivalent circuit modeling of graphene oxide solutions. *Nanomaterials* 7: 446. https://doi.org/10.3390/nano7120446
21. Magar HS, Hassan RY, Mulchandani A (2021) Electrochemical impedance spectroscopy (EIS): principles, construction, and biosensing applications. *Sensors* 21: 6578. https://doi.org/10.3390/s21196578
22. Chen P, Wang G, Li J, et al. (2024) Anticorrosion mechanism of FACs-GO hybrids in ER coatings by EIS and MD simulation. *Prog Org Coat* 186: 107996. https://doi.org/10.1016/j.porgcoat.2023.107996
23. Backes C, Abdelkader AM, Alonso C, et al. (2020) Production and processing of graphene and related materials. *2D Materials* 7: 022001. https://doi.org/10.1088/2053-1583/ab1e0a
24 Lunney JK, Van Goor A, Walker KE, et al. (2021) Importance of the pig as a human biomedical model. *Sci Transl Med* 13: eabd5758. https://doi.org/10.1126/scitranslmed.abd5758
25. Abasi S, Aggas JR, Garayar-Leyva GG, et al. (2022) Bioelectrical impedance spectroscopy for monitoring mammalian cells and tissues under different frequency domains: a review. *ACS Meas Sci Au* 2: 495–516. https://doi.org/10.1021/acsmeasuresciau.2c00033
26. Bera TK (2018) Bioelectrical impedance and the frequency dependent current conduction through biological tissues: a short review. *IOP Conference Series: Materials Science and Engineering*.

27. Ferrari AC, Basko DM (2013) Raman spectroscopy as a versatile tool for studying the properties of graphene. *Nat Nanotechnol* 8: 235–246. https://doi.org/10.1038/nnano.2013.46
28. Frerichs I, Hinz J, Herrmann P, et al. (2002) Regional lung perfusion as determined by electrical impedance tomography in comparison with electron beam CT imaging. *IEEE T Med Imag* 21: 646–652. https://doi.org/10.1109/TMI.2002.800585
29. Hellige NC, Meyer B, Rodt T, et al. (2012) In-vitro evaluation of contrast media for assessment of regional perfusion distribution by Electrical Impedance Tomography (EIT). *Biomed Eng Biomed Te* https://doi.org/10.1515/bmt-2012-4442
30. Qu G, Wang X, Liu Q, et al. (2013) The ex vivo and in vivo biological performances of graphene oxide and the impact of surfactant on graphene oxid's biocompatibility. *J Environ Sci* 25: 873–881. https://doi.org/10.1016/S1001-0742(12)60252-6
31. Faes T, Van Der Meij H, De Munck J, et al. (1999) The electric resistivity of human tissues (100 Hz-10 MHz): a meta-analysis of review studies. *Physiol Meas* 20: R1. https://doi.org/10.1088/0967-3334/20/4/201
32. Luo Y, Abiri P, Zhang S, et al. (2018) Non-invasive electrical impedance tomography for multi-scale detection of liver fat content. *Theranostics* 8: 1636–1647. https://doi.org/10.7150/thno.22233
33. Jasim DA, Murphy S, Newman L, et al. (2016) The effects of extensive glomerular filtration of thin graphene oxide sheets on kidney physiology. *ACS Nano* 10: 10753–10767. https://doi.org/10.1021/acsnano.6b03358
34. Wei XF, Grill WM (2009) Impedance characteristics of deep brain stimulation electrodes in vitro and in vivo. *J Neural Eng* 6: 046008. https://doi.org/10.1088/1741-2560/6/4/046008
35. Crone C, Olesen S (1982) Electrical resistance of brain microvascular endothelium. *Brain Res* 241: 49–55. https://doi.org/10.1016/0006-8993(82)91227-6
36. Butt AM, Jones HC, Abbott NJ (1990) Electrical resistance across the blood-brain barrier in anaesthetized rats: a developmental study. *J Physiol* 429: 47–62. https://doi.org/10.1113/jphysiol.1990.sp018243

AIMS Press